

# Incremental indexing and retrieval mechanism for scalable and robust shape matching

Shehzad Khalid \*

*Department of Computer and Software Engineering, Bahria University, Islamabad,  
44000, Pakistan*

---

## Abstract

Techniques for efficient and effective content-based image matching are becoming increasingly important with the widespread increase in digital image capturing systems. Shape of an object, represented by its contour, is one of the most important visual feature that is thought to be used by humans to determine the similarity of objects. The selected feature and its distance measure must be robust to different distortions such as noise, articulation, scale and rotation. Existing approaches provides invariance to these distortions at the cost of either the accuracy due to poor discrimination ability or the efficiency. In this paper, we present an effective representation of shape, using its boundary information, that is robust to arbitrary distortions and affine transformation. The contour representation of shape is converted into time series and is modeled using orthogonal basis function representations. Shape matching is then carried out in the chosen coefficient feature space resulting in efficient matching. The efficiency of shape matching is further improved by indexing the shape descriptors using hierarchical indexing structure. A novel distributed beam search based technique is proposed that operates on the indexing structure and ensures no false dismissal for a given  $k$ -NN query. Experimental evaluation demonstrates that the proposed shape representation and matching mechanism is robust, efficient and scalable to very large shape datasets.

*Key words:* Shape matching, dimensionality reduction, affine invariant matching, indexing and retrieval, shape distance, pruning.

*PACS:*

---

\* Corresponding author.

*Email address:* shehzad.khalid@hotmail.com (Shehzad Khalid).

## 1 Introduction

The prevalence of digital image capturing system has prompted much research activity aimed at the development of sophisticated techniques that enables content-based image search. A fundamental feature that determines the content-based similarity of images is the similarity of object's shape in the image. Shape matching generally looks for effective and perceptually important shape representation and distance measures that are invariant to many distortions including noise, rotation, articulation, scale, jag etc. Rotation invariance is relatively difficult to handle as compared to noise, translation and other distortions. Shape matching using any representation scheme normally gives good results if the two shapes are rotationally aligned. Much of the earlier research on shape matching achieve rotation invariance at the cost of accuracy [1] or efficiency [3][4][5][2]. Our ultimate goal is to generate efficient and accurate rotation-invariant features to compare shapes that are represented using closed planar contours.

Much of the earlier research in shape matching and recognition has focused only on the accuracy of shape matching and retrieval systems. Efficiency requirement is often ignored in the evaluation of shape matching techniques which is as important as accuracy. An accurate but inefficient retrieval system will not be appreciated due to online retrieval demands. Low computation complexity is an important characteristic of a good shape descriptor. We target efficiency in two ways: decreasing one to one shape matching complexity and allowing indexing.

Efficient shape matching can be achieved using low dimensional feature space representation of shapes. The selected dimensional reduction technique should transform the high dimensional image to compact feature space while retaining most of the characteristic structure of the original data. Related work within the data mining community on approximation schemes for indexing time series data is highly relevant to the parameterisation of contour-based representation of shapes. Shapes can be converted into time series by calculating distance of every point from the shape-centroid. This makes the indexing techniques for time series applicable to contour-based shape matching. For example, Discrete Fourier Transforms (DFT) [6][7], Discrete Wavelet Transforms (DWT) [8], Adaptive Piecewise Constant Approximations (APCA) [9], and Chebyshev polynomials [10] have been used to conduct similarity search in time series data. Sequential matching of query with all shapes in dataset using compact features may retrieve results in reasonable time for small to medium size datasets (number of samples  $< 10000$  ). However, for large datasets (number of samples  $\gg 10000$ ), even efficient matching using compact features is too slow. One of the important challenges is to devise search mechanism that is scalable to very large datasets.

The major contribution of this paper is a novel indexing and retrieval algorithm that significantly improves the efficiency of given matching algorithm whilst ensuring no false negatives. In this context, we define false negatives as samples that are not retrieved using indexed search but would have been retrieved using sequential search for a  $k$ -NN query using given distance function. We achieve efficient retrieval in large datasets by generating hierarchical indexing structure using compact feature representation of shapes. We apply time series modeling of contour-based shape representation to the problem of shape matching. Contours are modeled using function approximation techniques and matching of shape is carried out in the coefficient subspace. An efficient matching technique is presented that can match 2D shapes which are not rotationally aligned. The proposed technique is also robust to noise and different affine transformations. An incremental tree-based indexing structure is proposed that enables extremely efficient retrieval. The tree defines a hierarchical quantization obtained using recursive clustering of shapes in the dataset. The proposed indexing structure supports online insertion and deletion of shape samples from dataset which is critical for incremental indexing. A novel distributed beam search based retrieval algorithm is proposed that ensures no false negatives. This results in exact indexing and retrieval of shapes which will always retrieve identical results to the sequential search for a given  $k$ -NN query.

The remainder of the paper is organized as follows: We review some relevant background material in section 2. In section 3 we present some function approximation approaches to contour-based shape representation. Section 4 addresses the issue of rotation invariant shape matching without compromising on efficiency and accuracy. In section 5, a hierarchical structure is proposed for incremental indexing of shape datasets. A novel approach, referred to as Distributed Beam Search (DBS), for searching using proposed indexing structure is also presented. Experiments have been performed to provide a comprehensive evaluation of our proposed technique and its comparison with existing approaches. These experiments are reported in section 6. The paper concludes with a discussion and proposals for further work.

## 2 Background and related work

Shape descriptors are known to be useful candidates for content-based image indexing and retrieval schemes. Previous work has sought to represent shapes through shape context, shape signature, integral invariants, curvature, moments etc. Broadly speaking, these shape representation and matching techniques are classified into two classes: 1) contour-based that only exploit contour information and 2) region-based that incorporate all the pixels within the shape to generate shape descriptor.

The contour-based approaches are more common in literature as studies on human perception have shown that humans can recognize and discriminate shapes by their contour features. We consider only contour-based approaches here. Most of the contour-based shape representation generates a global representation of contour. Some of the global representations include shape context [12][13][11], shape signature [14], integral invariants [15] and differential invariants [17][16]. Shape matching using global approximation is a simple process that requires parameter distance such as euclidean distance [2] or raw point-space distance such as DTW [2][18], hausdorff distance [19] and correspondence-based shape matching [11][12][13]. Point-space distances are not suitable for online shape matching due to high computation costs associated with 2-D mapping of shapes. Some approaches [5][20] segment the contour into pieces and generate a piecewise representation of shapes. Piecewise approaches differ in the segmentation criteria to break contours into pieces and the modeling mechanism used to represent contour segments. Some of the piecewise approaches include polygon decomposition [5], smooth curve decomposition [20] and curvature decomposition [21]. The advantage of piecewise approaches is its ability to support partial matching and as a result dealing with the problem of partial occlusion. However, this merit of piecewise approaches comes with the disadvantage of complex and inefficient matching. Piecewise approaches do not capture global features of shape which is extremely important for shape recognition and discrimination.

Rotation invariance is critical for accurate shape matching and is hard to achieve as compared with invariance to other distortions [2][22]. There exists a variety of techniques that has been used for rotation invariant shape matching. Some approaches [23][24] make use of rotation invariant features including features associated to curvature and centroid distances, ratio of perimeter to area, circularity, convexity etc. These approaches achieve rotation invariance by compromising on the accuracy. Approaches using 1D time series representation of shapes has also been proposed [2][25][26][27][28]. Some of these approaches [27] achieve rotation invariance by selecting very few starting point (alignment to major axis) to obtain 1D time series representation of 2D shape. However, such alignment are very unreliable specially when there is no well defined major-axis and slight articulation in shape may have significant impact on rotation alignment. On the other extreme, some researchers proposed to use brute-force search over all possible rotation to identify the true alignment of shapes [25][2][26]. We need to shift one contour  $n$  times ( $n \gg 100$ ) where  $n$  is the number of points on the contour. The matching of one shape is carried out with  $n$  different alignments of the other shape which jeopardises the efficiency requirement of content-based image search and retrieval systems.

Much of the earlier research focus has been on accurate shape matching while giving scant attention to the efficiency issue. The issue of scaling of shape search to large databases remains open with most of the existing shape match-

ing methods. Recently, some of the research work such as [2][11][35], has addressed the issue of large datasets. Keogh et al. [2] proposed a wedge-based technique to perform exact indexing of shape datasets. A hierarchical wedge-based binary tree is constructed to be used later for pruning of irrelevant shapes during retrieval. However, the approach suggests using computationally expensive DTW for accurate matching between high dimensional contour-based representation of shapes and use brute force approach for rotational invariance. All these factors contribute towards higher retrieval times than desired in spite of using early abandoning technique for efficiency purposes. Mori et al. [11] proposed two pruning techniques to address the issue of efficient shape matching from large shape datasets. One of the approaches is based on sequential shape matching but using only a subset of shape features referred to as shape contexts and certain number of nearest neighbors are selected. Shape matching with complete set of shape contexts is then carried out only for the selected shape samples. The second pruning approach works by employing vector quantization on the shape contexts and replacing each shape context with the ID of the cluster that it belongs to. Lowe et al. [35] proposed an efficient search mechanism that matches shapes by searching k-d tree with the proposed "Best-Bin-First" based algorithm. Tan et al. [37] captures shape feature using centroid-radii model which enables their feature vector to be presented as a multidimensional data point. This enables the use of multidimensional tree based indexing structures such as R-tree, PR-tree etc. Although R-tree have been previously used for shape matching [36], its performance decreases in the presence of high-dimensional feature vector. Tan et al. proposed an extension of R-tree, namely Nested R-tree based indexing structure (NR-tree). NR-tree is a multi-layer tree structure where each layer is a collection of R-trees that indexes on a subset of the dimensions. This enables NR-tree to work well in the presence of high dimensions and multi-resolution querying. Graumen et. al. [38] proposed a hierarchical approach for image retrieval. They use same number of child nodes at each level without considering the number of samples represented by a particular parent node. Ignoring the distribution of data while generating the tree-based hierarchical quantization of data-space results in a very large and bushy tree which results in inefficient query making. Inverted files based indexing has also been used to index a high dimensional sparse vector based shape representations [39][40].

The contribution of this paper is to show that a low dimensional coefficient-based contour encoding scheme can be used more efficiently for shape searching and matching than previous approaches that rely on high dimensional representation of shapes. The parameter subspace representation of contours is also robust to the presence of different levels of noise and other distortions. An extremely efficient mechanism to achieve rotation invariance in shape matching without compromising on accuracy is proposed. A hierarchical tree based indexing structure is also presented that allows exact indexing using any feature space which has a mean. The indexing of shape features using proposed tree-

based approach further improves the efficiency of proposed shape matching mechanism.

### 3 Shape representation

In this section, we present our global contour-based shape representation scheme based on time series representation. The shapes are pre-processed so that all the shapes have same area of minimum bounded rectangle (MBR) of shape. Let  $A_{actual}$  be the area of shape's MBR and  $A_{desired}$  is the desired area of MBR, the shape is re-scaled by the factor equivalent to  $A_{actual}/A_{desired}$ . This pre-processing step will make our shape matching approach invariant to scale changes in shapes. The object contour  $C(O)$  is then extracted from pre-processed image which is defined by the point sequence:

$$C(O) = \{(x_1, y_1), (x_2, y_2), \dots, (x_n, y_n)\} \quad (1)$$

where  $(x_1, y_1)$  represents the location of the left-top point on the contour and  $n$  is the number of points on the contour.

The 2-D raw point-based feature vector  $C$  is converted into 1-D centroid distance  $CD$  based time series by mapping each point on the contour to the distance between the point and the shape's centroid as:

$$CD_t = \{\sqrt{((x_t - x_c)^2 + (y_t - y_c)^2)}\} \quad t = 1, 2, 3, \dots, n \quad (2)$$

where

$$x_c = \frac{1}{n} \sum_{t=1}^n x_t, \quad y_c = \frac{1}{n} \sum_{t=1}^n y_t \quad (3)$$

The scale variance in shape representation is taken care of by normalizing the distance vector  $CD$  as:

$$CD_t = \frac{CD_t - \mu}{\sigma} \quad t = 1, 2, 3, \dots, n \quad (4)$$

where  $\mu$  is the mean and  $\sigma$  is the standard deviation of the centroid distances in  $CD$ . The process of conversion of shape into 1-D time series representation is depicted graphically in Figure 1. A sample shape of fighter plane is shown in Figure 1(a). Figure 1(b) presents the projection of plane in  $C$  space with 'o' marker highlighting the starting (left-top) point on the contour. The process of generating 1-D time series from 2-D contour is highlighted in Figure 1(c).

The distances of every point on the contour to the centroid is represented as 1-D time series in  $CD$  space. The projection of shape in  $CD$  space is presented in Figure 1(d).

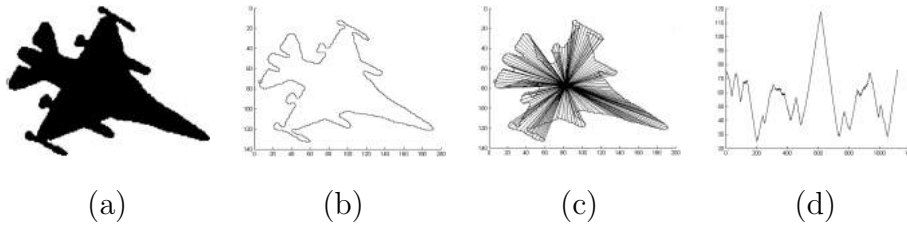


Fig. 1. Extracting 1D time-series representation of contour-based shapes. (a) Projection of shape in image plane. (b) Projection in  $C$  space with ‘o’ marker specifying the starting point (c) Mapping of contour from 2D  $C$ -space to 1D  $CD$ -space (d) Projection in  $CD$ -space.

For small objects with relatively simple shapes ( $n < 100$ ) it is feasible to work on raw centroid distance vector  $CD$ . However for realistic scenarios,  $n \gg 100$  and this renders direct manipulation of point sequence impractical for online retrieval purposes. The key to implementing efficient trajectory matching is dimensionality reduction. The idea is to determine a feature extraction function  $F$  that reduces the dimensionality of the data from  $n$  to  $m$  such that  $m \ll n$ . Similarity search and retrieval is then conducted in the reduced feature space. It is important that the feature space captures the most salient characteristics of the raw distance vector space. Influential work within the data mining community on indexing techniques for time series is highly relevant to the parameterisation of  $CD$ -space representation of shapes. For example, Discrete Fourier Transform (DFT) [6], Discrete Wavelet Transform (DWT) [8], Adaptive Piecewise Constant Approximation (APCA) [9], and Chebyshev polynomials [10] have been used to index time series and perform similarity retrieval.

We have employed Discrete Fourier Transform (DFT) to model the projection of shape in  $CD$  based time series representation. The  $n$ -point DFT of  $\{CD_i\}$ , defined as a sequence  $\{\overline{CD}_f\}$  of  $n$  complex numbers ( $f = 1, \dots, n$ ), is given as:

$$\overline{CD}_f = \frac{1}{\sqrt{n}} \sum_{i=1}^n CD_i \exp(-j2\pi fi/n) \quad f = 1, 2, \dots, n \quad (5)$$

where  $j$  is the imaginary unit  $j = \sqrt{-1}$ , and  $\overline{CD}_f$  are complex numbers with the exception of  $\overline{CD}_0$  which is real. As the centroid distance based time series is z-normalized,  $\overline{CD}_0$  which represents the mean of time series will always have a value of 0 and is ignored. Typically, the DFT sequence is truncated after  $m$  terms,  $f = 1, \dots, m - 1$ . In this case, the feature vector consists of  $2(m - 1)$  entries (from real and imaginary parts). More formally, let  $a_i$  and  $\hat{a}_i$  be the real and imaginary part of  $\overline{CD}$ . Shapes can be represented in the coefficient

feature space by a  $2(m - 1)$  dimensional vector of DFT coefficients  $\mathbf{F}_{DFT}$ , where

$$\mathbf{F}_{DFT} = [a_1, \hat{a}_1, \dots, a_{m-1}, \hat{a}_{m-1}] \quad (6)$$

The DFT based projection of 2D shapes results in consistent size ( $m$ ) feature vector irrespective of the number of points on the shape contour. The distance between two shapes is measured by calculating Euclidean distance between the DFT-based feature space representation of shapes. The selection of DFT for coefficient feature space representation of contour as compared to its competitive descriptors such as Chebyshev (CS)[10] and Piecewise Aggregate Approximation (PAA) [29] is justified through experimental evaluation as presented in section 6.

#### 4 Rotation Invariant Shape Representation

The mechanism specified in section 3 generates a centroid distance ( $CD$ ) based time series representation of shapes.  $CD$  is then converted into DFT-based coefficient feature space representation and shape matching is performed in the reduced feature space. This method produces good results if  $CD$ -based time series representation of two shapes are rotationally aligned. However, this method can produce poor results if the two shapes are not aligned. Existing techniques [2][3][4][25][26] solve this problem by keeping one shape fixed and rotating the other shape. The true distance between the shapes is the minimum of the distances of the fixed shape with all possible rotations of the other shape. This brute force approach, though effective, is extremely inefficient. Let  $n$  ( $n \gg 100$ ) be the length of  $CD$ -based representation of contour, then we need to calculate  $n$  shape distances to achieve a rotational invariant shape matching. This cripples one of our primary objective of efficient shape matching.

To overcome inefficiency in rotation invariant shape matching, we propose a Critical-point based approach for Rotational Invariant Shape Matching (CRISM). Instead of calculating the distance of fixed shape with all possible rotations of other shape, we rotate both the shapes along the selected number of critical points on the contour and use them as starting points to convert contour into  $CD$ -based time series representation. The number of critical points to be used for rotational alignment of shapes is dependant on the complexity of shape's contour and is different for different shapes. The critical points in the contours are extracted by identifying local maximas in  $CD$ -space. We have employed  $k$ -beam search to identify local maximas. The process of identifying critical points on the contour is highlighted in Figure 2. Figure 2(a) presents the  $CD$ -space representation of shape with critical points highlighted using ' $\Delta$ ' marker.

Figure 2(b) presents the 2D contour-based representation of shape with ‘ $\Delta$ ’ markers superimposed on critical points.

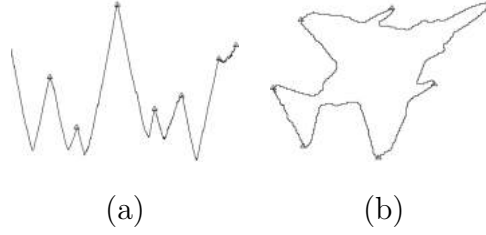


Fig. 2. Identification of critical points using local-maxima heuristic. Critical points are highlighted using ‘ $\Delta$ ’ marker (a) in 1D  $CD$ -space representation (b) in 2D contour-space representation

The distance between the two shapes is calculated by rotating both the shapes along their respective critical points. Lower dimensional representation of  $CD$ -based time series, corresponding to given rotations of the shapes, is generated and is used to compute distance between the two shapes w.r.t. a particular alignment. The critical rotation of the shapes that gives the minimum distance value will result into correct alignment of two shapes and will return the rotation invariant distance. Comparison of proposed critical-point alignment with computationally expensive brute-force alignment is presented in Figure 3. For different pair of shapes, the alignment obtained using brute-force alignment is no better than the alignment obtained using critical-point approach. The number of iterations required using brute force approach is  $2^n$  where  $n$  is the number of points on the curve. On the other hand, critical-point alignment requires  $2^{nc}$  iterations where  $nc$  is the number of critical points on the curve. As  $nc \ll n$ , we have managed to achieve efficient rotation invariance without compromising the accuracy of rotation invariance shape matching.

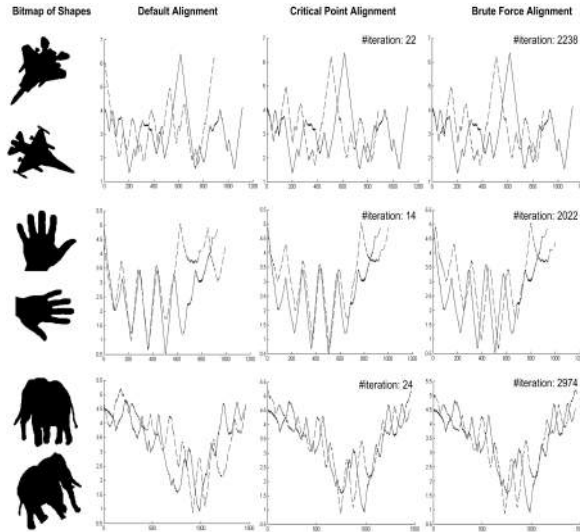


Fig. 3. Comparison of rotational invariant shape alignment using critical-point and brute-force alignment.

More formally, suppose we have a time series  $A$  representing a shape in  $CD$ -space as:

$$A = a_1, a_2, a_3, \dots, a_q \quad (7)$$

where  $q$  is the length of time series  $A$ . We identify a set of  $nc_A$  critical points  $C = \{c_1, c_2, \dots, c_{nc_A}\}$  using time series  $A$ . We achieve rotation invariance by expanding  $A$  into a matrix  $\mathbf{A}$  of  $nc_A$  time series as:

$$\mathbf{A} = \begin{bmatrix} a_{c_1}, \dots, a_{q-1}, a_q, a_1, \dots, a_{c_1-1} \\ a_{c_2}, \dots, a_{q-1}, a_q, a_1, \dots, a_{c_2-1} \\ \vdots \\ a_{c_{nc_A}}, \dots, a_{q-1}, a_q, a_1, \dots, a_{c_{nc_A}-1} \end{bmatrix} \quad (8)$$

Each row in matrix  $\mathbf{A}$  is a time series representing contour in  $CD$ -space aligned w.r.t. one of the critical point. To make our distance measure invariant to mirror images, we pad our matrix  $\mathbf{A}$  with the reverse of all the time series as:

$$\mathbf{A} = \begin{bmatrix} a_{c_1}, \dots, a_{q-1}, a_q, a_1, \dots, a_{c_1-1} \\ a_{c_2}, \dots, a_{q-1}, a_q, a_1, \dots, a_{c_2-1} \\ \vdots \\ a_{c_{nc_A}}, \dots, a_{q-1}, a_q, a_1, \dots, a_{c_{nc_A}-1} \\ a_{c_1-1}, \dots, a_1, a_q, a_{q-1}, \dots, a_{c_1} \\ a_{c_2-1}, \dots, a_1, a_q, a_{q-1}, \dots, a_{c_2} \\ \vdots \\ a_{c_{nc_A}-1}, \dots, a_1, a_q, a_{q-1}, \dots, a_{c_{nc_A}} \end{bmatrix} \quad (9)$$

The proposed framework for rotational invariant shape matching also supports partial rotational invariance where we only want to allow limited rotation in shape matching. This can be achieved by rotating one of the shape along

limited number of critical points. This can be specified as:

$$\mathbf{A} = \begin{bmatrix} a_{c_1}, \dots, a_{q-1}, a_q, a_1, \dots, a_{c_1-1} \\ a_{c_2}, \dots, a_{q-1}, a_q, a_1, \dots, a_{c_2-1} \\ \vdots \\ a_{c_i}, \dots, a_{q-1}, a_q, a_1, \dots, a_{c_i-1} \\ a_{c_{(nc_A-i+1)}-1}, \dots, a_1, a_q, a_{q-1}, \dots, a_{c_{(nc_A-i+1)}} \\ a_{c_{(nc_A-i+2)}-1}, \dots, a_1, a_q, a_{q-1}, \dots, a_{c_{(nc_A-i+2)}} \\ \vdots \\ a_{c_{nc_A}-1}, \dots, a_1, a_q, a_{q-1}, \dots, a_{c_{nc_A}} \end{bmatrix} \quad (10)$$

where  $i < (\frac{nc_A}{2})$ .

Let  $B$  be the time series representing some other shape in  $CD$ -space,  $C = \{c_1, c_2, \dots, c_{nc_A}\}$  be the set of  $nc_B$  critical points identified using time series  $B$  and  $\mathbf{B}$  be a feature matrix of  $B$  as obtained using eq. (10) using corresponding critical points for  $B$ . The rotational invariant distance between shapes  $A$  and  $B$  can then be specified as:

$$RID(\mathbf{A}, \mathbf{B}) = \min_{1 \leq i \leq nc_A} \min_{1 \leq j \leq nc_B} (DIST(DFT(A_{c_j}), DFT(B_{c_i}))) \quad (11)$$

where  $DFT(\cdot)$  is DFT based dimensionality reduction function and  $DIST(\cdot, \cdot)$  is the distance measure. The distance function commonly used for matching coefficient feature space representation of shape is euclidean distance. However, DTW can also be used to match PAA based coefficient feature space representation of shapes. For euclidean distance, the time complexity of querying a shape database using CRISM algorithm is  $O(2 * nc_A * nc_B * m * N)$  where  $nc_A$  and  $nc_B$  are the number of critical points,  $m$  is the size of feature vector used for shape representation and  $N$  is the number of samples in a shape dataset. However, the number of critical points rarely exceeds 15 even for complex shapes and the value of  $m$  is on the order of 8 to 32.

## 5 Hierarchical Tree-Based Indexing and Retrieval

Given a very large shape dataset, it is very difficult to meet online retrieval demands even in coefficient feature space representation due to sequential matching of query shape with all shapes in the dataset. To solve this problem, we wish to quickly filter distant shapes and identify a short list of candidate

shapes that includes the  $k$ -nearest neighbours of the query. Shape matching should then be carried out with the identified subset of candidate shapes. In this section, we propose a hierarchical tree based indexing and retrieval technique that addresses this issue. The tree basically defines a hierarchical quantization obtained using recursive clustering of shapes in the dataset. The algorithms for major operations on the tree including creation, updation and search are presented in following subsections.

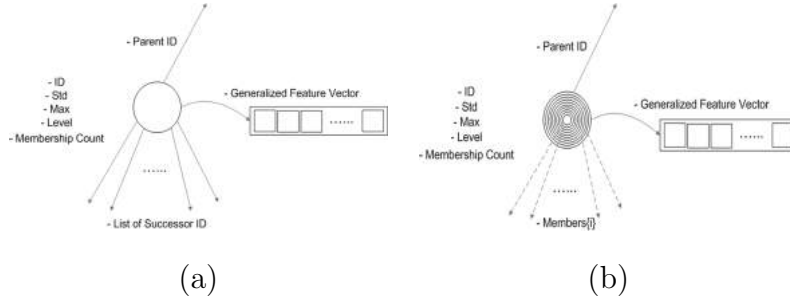


Fig. 4. Depiction of node data structures in the indexed tree for (a) non-leaf nodes (b) leaf nodes.

### 5.1 Building Hierarchical Index Structure

The proposed algorithm for creating shape-database index is a tree-based indexing mechanism that takes the entire set of shapes and attempts to determine  $b^*$  groupings in the dataset. Each grouping is represented by a node data structure in the tree. Each node has a parent, a state represented by a generalized feature vector representation of the shapes and other bookkeeping fields. The node data structure for non-leaf and leaf nodes are depicted in Fig. 4. Details of different bookkeeping fields in node data structures are presented in Table 1. If the membership count of any node exceeds a membership threshold, the node split occurs. This is done by identifying further  $b^*$  groupings from the subset of shape represented by the node. The process is repeated until the membership count of none of the node exceeds the membership threshold.

The identification of hierarchical groupings to generate tree-based indexing structure is based on iterative SOM-based clustering algorithm which comprises the following steps:

- (1) Initialize SOM network with the  $b^*$  output nodes.
- (2) Estimate mean ( $\mu$ ) and covariance ( $\Sigma$ ) of DFT-based coefficient feature space representation of shapes in  $DB$  using their default alignment. Initialize weight vectors  $W_i$  (where  $1 \leq i \leq \#_{output}$ ) from the  $PDF N(\mu, \Sigma)$ .
- (3) Sequentially input feature vectors from  $DB$  and identify  $k$  Nearest Weights ( $k$ -NW) to input feature vector using:

Bookkeeping field	Symbol	Description
ID	$ID$	Identity number to uniquely identify the node.
Parent ID	$parent\_ID$	Identity number of the parent node which later be used for bottom-up parsing of tree.
Level	$l$	Depth level of the node in the tree.
Generalized Feature Vector	$\overline{W}$	Stores the descriptor feature vector representation of the group (represented by the node) that is closest to the group center.
List of Successor ID	$successors$	Bookkeeping field of non-leaf nodes that stores the list of pointers (represented by solid arrows) of the child nodes which will later be used for top-down parsing of tree.
List of members shape	$members\{i\}$	Bookkeeping field of leaf nodes that stores the list of pointers (represented by dashed arrows) of the shape IDs indexed by the leaf node. Within the node, members are further grouped into $i = \{1, \dots, p\}$ bins (represented by rings in Figure 4b) w.r.t. the distance of sample from the generalized feature vector to improve pruning power. Bin 1 is closest and bin $p$ is furthest from node center.
Max statistic	$max$	Specifies the maximum of the distance of all the member shape samples from the generalized feature vector of the node.
STD statistic	$std$	Specifies the standard deviation of the distance of all member shape samples from the generalized feature vector of the node.
Membership count	$count$	Total number of members indexed with the node of the tree.

Table 1

Description of bookkeeping fields in the node data structure.

$$k - NM(\mathbf{A}, \mathbf{W}, k) = \{\mathbf{C} \in \mathbf{W} | \forall R \in \mathbf{C}, S \in \mathbf{W} - \mathbf{C}, \\ RID(R, \mathbf{A}) \leq RID(S, \mathbf{A}) \wedge |\mathbf{C}| = k\} \quad (12)$$

where  $\mathbf{W}$  is the set of all weight vectors,  $C$  is the set of  $k$  closest weight vectors and  $RID(R, \mathbf{A}) = \min_{1 \leq i \leq n_c} (DIST(R, A_{c_i}))$ . The value of  $k$  determines the number of output nodes that are nearest to  $\mathbf{A}$  and will be updated in the specific iteration of learning process. For a given training cycle  $t$ ,  $k = \delta(t)$  where  $\delta(t)$  is a neighborhood size function.

- (4) Train SOM network by adjusting a subset of weight vectors ( $C$ ) using

$$W_c(t+1) = W_c(t) + \alpha(t)\zeta(j)(F - W_c(t)) \quad \forall W_c \in C \quad (13)$$

where  $W_c$  is the weight vector representation of output node  $c$ ,  $j$  is the order of closeness of  $W_c$  to  $F$  ( $1 \leq j \leq k$ ),  $\zeta(j, k) = \exp(-(j-1)^2/2k^2)$  is a membership function,  $\alpha(t)$  is the learning rate of SOM and  $t$  is the training cycle index.

- (5) Decrease the learning rate  $\alpha(t)$  and neighborhood size  $\delta(t)$  exponentially over time.
- (6) Repeat steps 4-6 for all the training iterations. The resultant weight vectors are the cluster center representation for the  $b^*$  groupings in a given set of shapes.
- (7) Generate  $b^*$  nodes to represent  $b^*$  groupings and set:

$$\begin{aligned} \Gamma_i.\overline{W} &= W_i \\ \Gamma_i.max &= \max_{\forall \mathbf{A} \in \Gamma_i} (RID(\Gamma_i.\overline{W}, \mathbf{A})) \quad \text{for } i = 1, \dots, k \\ \Gamma_i.std &= \sum_{\forall \mathbf{A} \in \Gamma_i} (RID(\Gamma_i.\overline{W}, \mathbf{A}) / |\Gamma_i|) \end{aligned} \quad (14)$$

where  $\Gamma$  is the node structure and  $|\Gamma_i|$  is the membership count of  $\Gamma_i$ . Add these nodes in the index tree as the successor (child nodes) of the parent node.

- (8) Terminate the algorithm if the indexing process is stable. The tree-based indexing structure is considered stable if the membership count of none of the identified grouping is greater than a cluster membership threshold  $\kappa$ . The validation process can be specified as:

$$\hat{\Gamma} = \{\Gamma_i \in \Gamma \mid |\Gamma_i| > \kappa\} \quad \forall i \quad (15)$$

If the indexing process is unstable ( $\hat{\Gamma} \neq \{\}$ ), the subset of shapes represented by cluster  $\Gamma \in \hat{\Gamma}$  is treated as another set of shapes. The algorithm goes to step (1) and attempts to identify further  $b^*$  groupings in the given set of shapes.

Depiction of hierarchical tree-based indexing structure, generated using the proposed indexing algorithm, for indexing of large shape datasets is presented in Figure 5. Blob area of each node represents its membership count. Solid arrows represents the link from the parent to the child node of the tree where as dotted arrow represents the link from the leaf node to its indexed subset of shapes in the dataset. The proposed top-down approach for hierarchical index structure is more efficient than the alternative bottom-up approach. The time complexity of generating hierarchical index structure using top-down approach is  $O(l * b^* * N)$  instead of  $O(b^{*l} * N)$  for bottom-up approach where  $N$  is the number of training iterations.

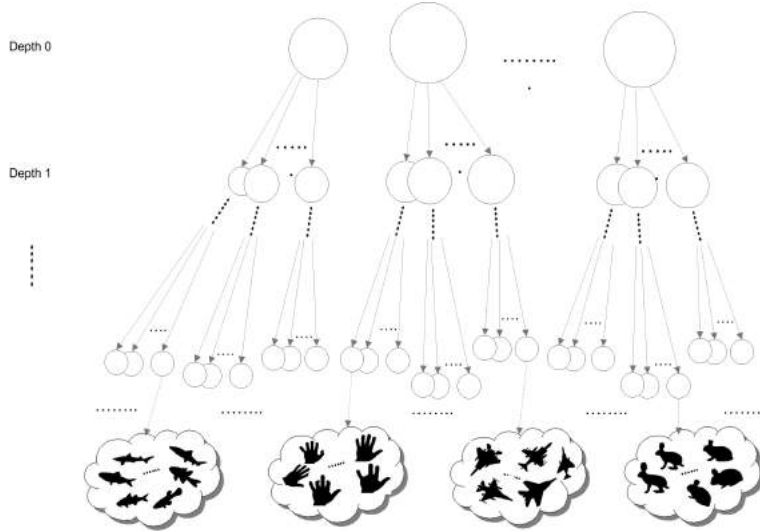


Fig. 5. Depiction of a hierarchical tree-based indexing structure generated using proposed indexing mechanism.

## 5.2 Updating Hierarchical Index Structure

One of the important operation on the indexing structure is updation which is critical for incremental indexing of shapes. The main aim of updation is to insert or remove shapes from the indexed dataset without the requirement of re-building the index structure all over again which is computationally expensive for gigantic datasets. The proposed hierarchical tree-based index structure is flexible to any updates caused by insertion or deletion of shape samples in the database.

### 5.2.1 Insertion Algorithm

The algorithm for insertion of new shapes in the indexed dataset and updation of hierarchical tree-based index structure comprises the following steps

- (1) Generate matrix-based feature vector representation ( $\mathbf{A}$ ) of shape to be inserted in the indexed dataset
- (2) Initialize candidate search list  $\Gamma$  with the nodes present at level 0 of the tree.
- (3) Classify the sample shape to one of the nodes from  $\Gamma$ . This is done by calculating the rotational invariant distance (RID) between the sample shape and the weight vectors associated to each node in the search list and identify the closest node as:

$$c = \arg \min_k RID(\Gamma_k \cdot \overline{W}, \mathbf{A}) \quad \forall k \quad (16)$$

where  $\Gamma_k \cdot \overline{W}$  is the weight vector associated to node  $\Gamma_k$

- (4) Check the validity of classification process. The classification of sample shape to node  $\Gamma_c$  is considered to be valid if:

$$RID(\Gamma_c.\overline{W}, \mathbf{A}) \leq \max(\Gamma_c.max, 3 * \Gamma_c.std) \quad (17)$$

- (5) If the condition specified in eq. (17) is satisfied and  $\Gamma_c$  is a non-leaf node, set candidate list  $\mathbf{\Gamma}$  to the successors (children nodes) of  $\Gamma_c$ . Go to step (3).
- (6) If the condition specified in eq. (17) is satisfied and  $\Gamma_c$  is a leaf node, index the shape with the  $ID$  of  $\Gamma_c$  and update the  $max$  and  $std$  statistic associated to  $\Gamma_c$ . If the membership count of  $\Gamma_c$  gets greater than  $\kappa$ ,  $\Gamma_c$  becomes unstable and is split into  $b^*$  child nodes by using the algorithm specified in section 5.1. Subset of shapes from  $DB$  that are indexed with  $\Gamma_c$  are used for sub-tree generation.
- (7) If the condition specified in eq. (17) is not satisfied, generate a new node  $\Gamma_{new}$  at the depth level equivalent to  $\Gamma_c.l$ . Set  $\Gamma_{new}.parent\_ID = \Gamma_c.parent\_ID$  and set  $\Gamma_{new}.\overline{W}$  to the feature vector associated to the default alignment of the shape. The shape is then indexed with the  $ID$  of  $\Gamma_{new}$  and is inserted into the database.
- (8) After inserting all the shapes as a batch into the database, update the generalized weight vector representation ( $\overline{W}$ ) corresponding to the updated nodes. This is done by finding the alignment of all member shapes of the node with the generalized weight vector representation. The generalized weight vector is then updated with the mean value of the DFT-based coefficient feature space representations of aligned shapes.

### 5.2.2 Deletion Algorithm

The algorithm for removing shapes from the dataset and updation of hierarchical tree-based index structure comprises the following steps

- (1) Remove the shape ID from the *members* field of the leaf node with which the shape is indexed.
- (2) If the leaf node contains more members, recursively update the book-keeping fields (max, STD and membership count statistics) of the leaf-node and its parent nodes.
- (3) If the leaf node does not contain any member, remove the leaf node and update the successor list of its parent node. If the successor list of parent node gets empty, remove the node and update its corresponding parent. Repeat this process till the successor list of the parent node is a non-empty list.
- (4) After deleting all the shapes as a batch from the database, update the generalized weight vector representation ( $\overline{W}$ ) corresponding to the updated nodes as specified in step (8) of Insertion algorithm.

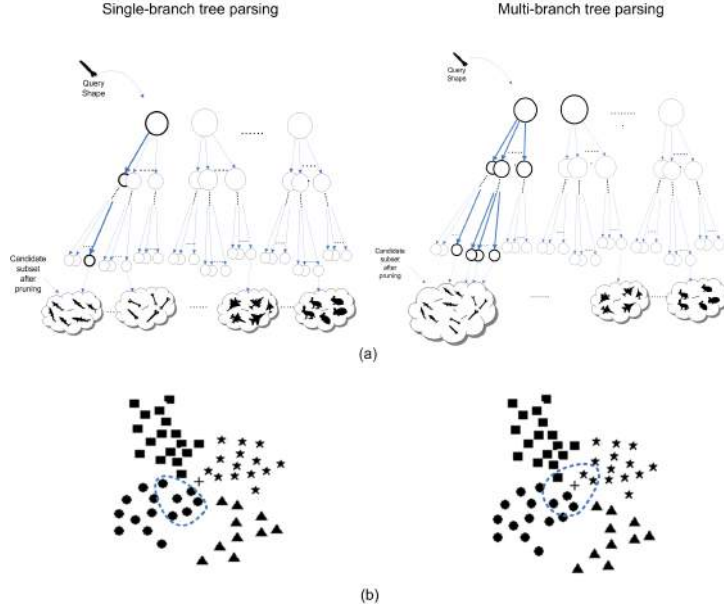


Fig. 6. Depiction of  $k$ -NN query using single-branch and multi-branch parsing of hierarchical index structure in (a) tree-based indexing space (b) simulated 2D space.

### 5.3 Retrieval Algorithm

This section presents a retrieval algorithm to search  $k$ -NN of the query shape using index tree structure while ensuring no false negatives. The basic idea of the algorithm is to exploit multiple paths instead of moving along single branch of the tree in order to exploit all possible nodes that may contain the desired result of query shapes. Parsing the index tree using single branch will give correct results if the query shape is closer to the generalized feature vector representation of the selected nodes along the tree-based indexing structure. However, if the query shape lies at the boundary of different groupings of shapes indexed by different nodes, the desired results can not be achieved. This phenomena is highlighted in Figure 6. Figure 6(a) and Figure 6(b) depicts the problem of single-branch parsing and its possible solution using multi-branch parsing in tree-based indexing space and in 2D simulated space respectively. Single-branch parsing selects only one node at each level of the tree where as the desired query result may contain shapes that are indexed by different nodes. This will result in the presence of false negatives in the candidate search list thus effecting the search results. The problem can be solved by parsing through multiple branches to select all nodes that may contain subset of shapes of the desired result. Figure 6(b) presents the simulation of this phenomena in 2D space for ease of visualization and understanding. Each point in the plot is representing a shape in 2D space and shape indexed with same node id is represented with similar marker. Points enclosed in dashed ellipse represents the search results for the query represented by ‘+’ marker.

The proposed retrieval approach, referred to as Distributed Beam Search (DBS), make use of this multi-branch parsing method. The algorithm dynamically checks the eligibility of nodes to be included in search at different levels of index tree structure. The algorithm for  $k$ -NN retrieval using proposed DBS technique comprises the following steps:

- (1) Generate matrix-based feature vector representation ( $\mathbf{A}$ ) of the query shape.
- (2) Initialize candidate search list  $\mathbf{\Gamma}$  with the nodes present at depth level 0 of the tree.
- (3) Sort  $\mathbf{\Gamma}$  in ascending order with respect to the distance of generalized feature vector representation of all nodes  $\Gamma \in \mathbf{\Gamma}$  from query  $\mathbf{A}$ .
- (4) Identify subset of nearest nodes from query shape as:

$$\mathbf{\Gamma}_i = \{ \{ \Gamma_1, \Gamma_2, \dots, \Gamma_p \} \in \mathbf{\Gamma} \mid \sum_{i=1}^p \Gamma_i.count \geq k \wedge \sum_{i=1}^{p-1} \Gamma_i.count < k \} \quad (18)$$

where  $p$  is the index of most distant node from query shape in  $\mathbf{\Gamma}_i$ .

- (5) Identify second subset of nodes from  $\mathbf{\Gamma}$  to ensure no false negatives as:

$$\mathbf{\Gamma}_j = \{ \Gamma_i \in \mathbf{\Gamma} \mid (RID(\Gamma_i.\overline{W}, \mathbf{A}) - \Gamma_i.max) \leq (RID(\Gamma_p.\overline{W}, \mathbf{A}) + \Gamma_p.max) \} \quad \forall i \quad (19)$$

- (6) Set  $\mathbf{\Gamma} = \mathbf{\Gamma}_i \cup \mathbf{\Gamma}_j$ .
- (7) If there are non-leaf nodes in  $\mathbf{\Gamma}$ , replace them with their child nodes. Repeat steps 3-7 till there are no leaf nodes in  $\mathbf{\Gamma}$ .
- (8) Retrieve the feature vector representation of all the shapes that are indexed by nodes present in  $\mathbf{\Gamma}$  satisfying the following condition:

$$RID(\Gamma_i.\overline{W}, \mathbf{A}) \leq (RID(\Gamma_p.\overline{W}, \mathbf{A}) + \Gamma_p.max) \} \quad \forall \Gamma_i \in \mathbf{\Gamma} \quad (20)$$

- (9) For the nodes that do not satisfy condition specified in eq. (20), retrieve only subset of shapes that belong to the outer rings of the nodes whose distance from query sample  $\mathbf{A}$  is less than  $(RID(\Gamma_p.\overline{W}, \mathbf{A}) + \Gamma_p.max)$ . The process of retrieval of shapes indexed by nodes in  $\mathbf{\Gamma}$  is highlighted in Figure 7. The query sample in state space is represented by ‘+’ marker. The blob area of each node represents the max statistics and the ring represents the bins within each node based on the distance from node center. The samples lying in shaded region of the state space is selected for sequential matching with query shape.
- (10) Let  $DB_{pruned}$  be the set of samples retrieved in steps (8) and (9), identify  $k$ -NN to query  $\mathbf{A}$  using:

$$k - NN(\mathbf{A}, DB_{pruned}, k) = \{ \mathbf{C} \in DB_{pruned} \mid \forall R \in \mathbf{C}, S \in DB_{pruned} - \mathbf{C}, RID(R, \mathbf{A}) \leq RID(S, \mathbf{A}) \wedge |\mathbf{C}| = k \} \quad (21)$$

where  $R$  and  $S$  are matrix-based feature vector representation of shapes in  $DB_{pruned}$ .

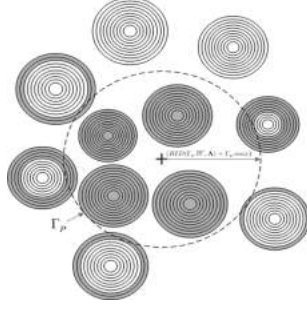


Fig. 7. Depiction of pruning with proposed DBS-based retrieval using ring structure of leaf nodes.

**Proposition1.** The proposed indexing and retrieval technique will always retrieve identical results to the sequential search for a given  $k$ -NN query.

*Proof.* The membership region of each node in the index tree can be visualized as a hyper sphere. The simplest case of  $k$ -NN retrieval of a given query sample is when the sample lies at the center of the hypersphere of a certain node and the number of members of the node is greater than  $k$ . In this particular case, we need to select only one node to achieve exact indexing of shape. However, we will prove the exact indexing capacity of our proposed approach by taking the worst case where each sample to be retrieved is indexed by a different node. We will prove that the proposed algorithm ensures the selection of all such nodes in the candidate list.

Let  $p$  be the index of the most distant node from query sample in set  $\Gamma_i$  as identified in eq. (18). The samples indexed by nodes present in set  $\Gamma_i$  contains at least  $k$ -neighbors of the query sample  $Q$ . However, we are not sure that these  $k$ -neighbors are the  $k$ -nearest neighbors of the query. To ensure no false negatives, we need to include all the nodes that may contain a sample whose distance from the query is less than the distance of the farthest of the  $k$ -neighbors, referred to as  $D_k$ . The upper bound on  $D_k$  can be specified as:

$$D_k \leq DIST(\Gamma_p.\bar{W}, \mathbf{Q}) + \Gamma_p.max \quad (22)$$

where  $DIST(.,.)$  is the distance function used with the hierarchical indexing and retrieval mechanism. Let  $D_k^*$  be the distance of the  $k^{th}$  nearest neighbour of the query sample, then

$$D_k^* \leq D_k \quad (23)$$

Using eq.(22) and (23)

$$D_k^* \leq DIST(\Gamma_p.\bar{W}, \mathbf{Q}) + \Gamma_p.max \quad (24)$$

A node  $\Gamma_i$  can index one of the  $k$  nearest neighbours of the query if and only if:

$$DIST(\Gamma_i.\overline{W}, \mathbf{A}) - \Gamma_i.max \leq D_k^* \quad (25)$$

Using eq. (24) and (25), we have

$$DIST(\Gamma_i.\overline{W}, \mathbf{A}) - \Gamma_i.max \leq DIST(\Gamma_p.\overline{W}, \mathbf{Q}) + \Gamma_p.max \quad (26)$$

Since  $k$ -beam search ensures the selection of all the nodes that satisfy the condition specified in eq. (26), it therefore guarantees no false negatives.

## 6 Experimental Results

This section analyzes the performance of the proposed shape matching approach with respect to the accuracy and efficiency requirement in the presence of increasingly large shape databases. The experiment has been conducted on variety of shape datasets including silhouette dataset<sup>1</sup>, projectile points and heterogenous dataset [2], chicken pieces dataset [43], MixedBag dataset<sup>2</sup> [2] and Diatoms dataset<sup>3</sup> [2].

### 6.1 Experiment 1: Performance evaluation of dimensionality reduction techniques

The purpose of this experiment is to investigate the robustness of DFT-based dimensionality reduction technique (DR) to the real life problem of noise and other distortions in shapes as compared to its competitive techniques including Chebyshev (CS)[10] and Piecewise Aggregate Approximation (PAA) [29]. The experiment has been conducted on noisy shapes from silhouette dataset. We have randomly selected six samples from each of the shape categories that are present in the dataset. The evaluation metrics used for the comparison of various DR techniques and distance measures are Exact Retrieval Accuracy (ERA) and Class Retrieval Accuracy (CRA). In the context of the current experimental evaluation, ERA can be defined as the ratio of the number of 1-NN queries that retrieve the desired result to the total number of queries.

<sup>1</sup> Silhouette dataset is available at: <http://www.lems.brown.edu/vision/researchAreas/SIID/silhouette-database.tar.gz>

<sup>2</sup> MixedBag dataset is available at: <http://www.cs.ucr.edu/~eamonn/shape/shape.htm>

<sup>3</sup> Diatom dataset is available at: <http://rbg-web2.rbge.org.uk/ADIAC/>

CRA can be defined as the ratio of the number of correct closest matches in 6-NN queries that retrieve the desired result to the total number of retrievals.

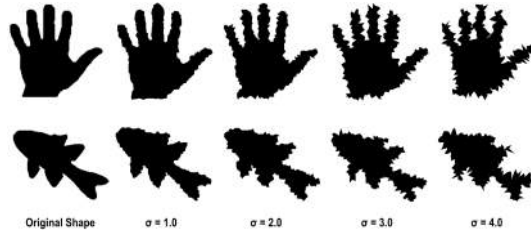


Fig. 8. Effect of simulated noise using increasing value of  $\sigma$  on sample shapes.

The silhouette dataset provides ground truth (i.e. manually labelled) shapes and so we try to simulate the effects of noise. A dataset is corrupted by moving all points on the contour in the normal direction by a certain distance  $d$  which determines the amount of noise that is induced in the shape. The value of  $d$  is generated from a zero-mean gaussian distribution and standard deviation of  $\sigma$ . If  $\mathbf{S}$  represents the original data, a noise corrupted dataset  $\mathbf{S}_C$  is produced by adding the term  $N[0, \sigma]$  to each  $(x, y)$  coordinate on the contour in the normal direction. We set  $\sigma = \{1.0, 2.0, 3.0, 4.0\}$  to simulate different noise levels. Simulation of different level of noise on two shapes is presented in Figure 8. Coefficient feature vector of contours in  $\mathbf{S}$  and  $\mathbf{S}_C$  are generated separately using DFT, CS and PAA. Each corrupted trajectory in  $\mathbf{S}_C$  is then selected as an example query  $Q_C$  and we search for a set of  $k$  nearest matches in the original dataset  $\mathbf{S}$ . This is defined as:

$$k - NN(Q_C, \mathbf{S}, k) = \{\mathbf{R} \in \mathbf{S} | \forall A \in \mathbf{R}, B \in \mathbf{S} - \mathbf{R}, \\ RID(A, Q_C) \leq RID(B, Q_C) \wedge |\mathbf{R}| = k\} \quad (27)$$

For ERA-based evaluation metric, we set  $k = 1$  in eq. (27). A set of rankings  $\forall Q_C \in \mathbf{S}_C$  is produced. The closest match to  $Q_C$  should be its corresponding uncorrupted version in  $\mathbf{S}$  which produces a rank value of unity. For ease of comparison we record the proportion of times (as a percentage) the query shape is ranked correctly as unity when taken over all  $S_C$ . For CRA-based evaluation metric, we set  $k = 6$  in eq. (27) as there are six members in each shape class. A set of rankings  $\forall Q_C \in \mathbf{S}_C$  is produced. A rank value for each 6-NN query is calculated as a percentage of the correct closest matches in nearest six matches. ERA percentage is then the average rank values for  $\forall Q_C \in \mathbf{S}_C$ .

For comparison of distance metrics, we have selected euclidean distance (ED) and DTW as  $DIST(.,.)$  function in eq. (12) for rotational invariant shape matching. We have used DTW as a distance metric for only PAA based feature vector representation of shapes as it can not handle feature space obtained using transformed global approximations. ED can work with both the original and transformed feature subspace and has been used as a distance metric for CS, DFT and PAA based representation. The experiment is repeated for

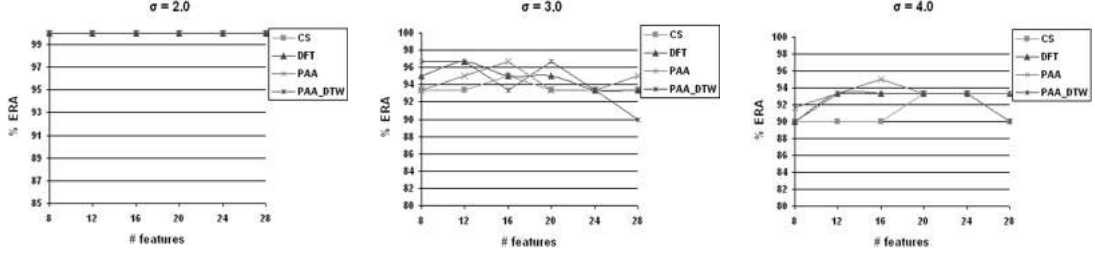


Fig. 9. Effect of different level of noise on exact retrieval accuracy (ERA) using different dimensionality reduction techniques and distance measures.

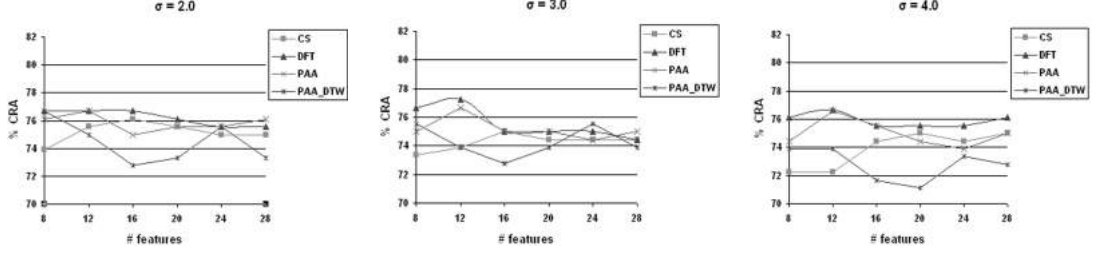


Fig. 10. Effect of different level of noise on class retrieval accuracy (CRA) using different dimensionality reduction techniques and distance measures.

different number of coefficients ( $\#_{features}$ ) in CS, PAA and DFT and for various values of  $\sigma$ . The results using ERA metrics are summarised in Figure 9. The figure consists of three separate graphs for the standard deviation of  $\sigma \in \{2.0, 3.0, 4.0\}$ . In all cases, varying the size of the feature vector is shown on the  $x$ -axis and the  $y$ -axis shows the average retrieval accuracies obtained using different dimensionality reduction schemes and distance measures. The experiment is repeated with the CRA metric and the results obtained are shown in Figure 10.

For ERA-based evaluation, PAA and DFT performs better than CS for higher noise levels (i.e.  $2.0 < \sigma < 4.0$ ), . For PAA, this is explained by the fact that PAA is an averaging scheme. As the noise induced is uniform on either side of the points on the contour, averaging over an interval has a cancelling effect of the noise. For DFT, good retrieval accuracy is explained by the property of distance preserving transform. CS does not give good retrieval accuracies and its performance degrades with increasing noise levels as compared to PAA and DFT. For CRA-based evaluation as presented in Figure 10, DFT performs consistently better than other dimensionality reduction techniques followed by PAA . It can also be observed from Figure 9 that PAA using ED gives better retrieval accuracy as compared to PAA using DTW ( $PAA_{DTW}$ ). Although DTW is useful in situations where time series have local time shifting but this benefit comes at the cost of increasing sensitivity to noise. DTW caters for time shifting by duplicating elements to ensure different parts of the time series can correspond. This aspect makes DTW noise-sensitive as outliers may be duplicated as well resulting into the degradation of performance of DTW

in the presence of noise.

Overall, the experiment demonstrates that DFT is a better choice for feature space representation of shape contours as compared to its competitive techniques. It is fairly robust to varying amounts of noise and other distortions as compared to PAA and CS specifically when evaluated with respect to class retrieval accuracy (CRA). A comparison of different distance measures in the presence of noise and other distortions, showed that ED in feature space is a better choice for similarity search than DTW. This justifies our selection of using DFT as a feature space representation and ED as a similarity metric in contour-based shape matching.

## 6.2 Comparison of CRISM with Competitive Techniques

The purpose of this experiment is to compare the performance of proposed CRISM-based approach for shape matching with competitive techniques. To establish a base case, we have implemented two different systems for comparison including integral invariants and differential invariants. The experiment has been conducted on silhouette dataset. For the proposed approach, shapes from the silhouette dataset are modeled using DFT-based coefficient feature vector. We assume  $m = 7$  in eq. (6) based on the comparative evaluation in experiment 1. The implementation of integral-invariants for shape modeling and matching is based on the adaptation of local-area integral invariants [15]. The implementation of differential invariants is based on the adaptation of curvature invariants [16][17]. Comparative evaluation is provided in terms of ERA and CRA metrics. Average ERA and CRA based retrieval accuracies for varying amount of noise in silhouette dataset are presented in Figure 11. The results from Figure 11 shows that CRISM gives the highest retrieval accuracies in the presence of different noise levels followed by integral invariants. Differential invariants performs worst in the presence of noisy shapes and its performance deteriorates with increasing noise levels.

To highlight the robustness of CRISM to noise and other distortions as compared to integral and differential invariants, the results of retrieving noisy shapes from a subset of silhouette dataset are presented in graphical format in Figure 12 for ease of visualization. Noisy query shapes are presented along the left column and the dataset is presented along the top row. The diagonal entries show the distance of noisy query shape with its corresponding non-noisy shape and the non-diagonal entries presents the distance of noisy shapes with other samples. Lower gray levels represent low distances and vice versa. Ideally, we want to have a a block diagonal structure with low gray levels along the diagonal. CRISM presents the best block diagonal structure followed by integral-invariant. Differential invariant presents high distances on the diago-

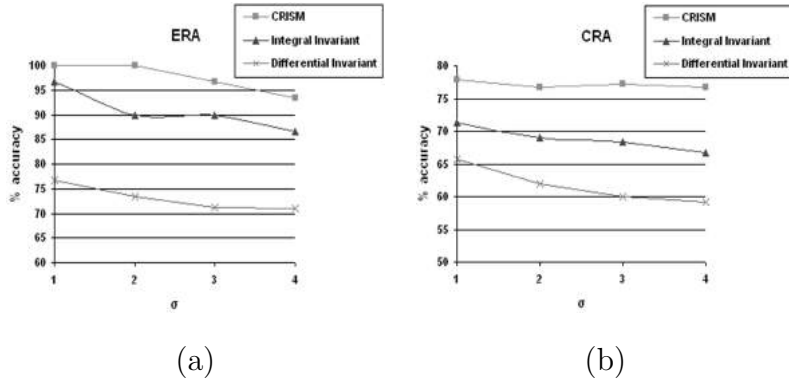


Fig. 11. Effect of different level of simulated noise on shape retrieval accuracy using (a) ERA metric (b) CRA metric

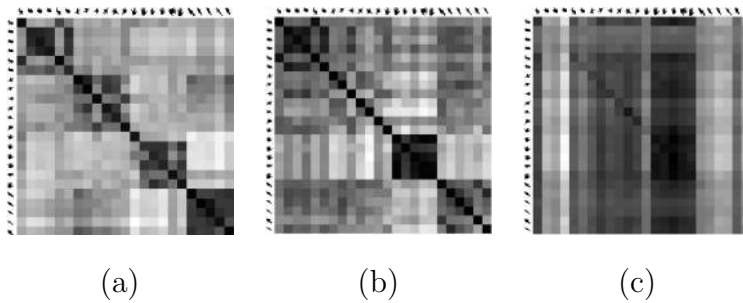


Fig. 12. Shape distances calculated between noisy shapes (left column) and original shapes (top row) using (a) proposed approach (b) integral invariant approach (c) differential invariant approach. Higher gray levels (lighter shades) represent high distances and vice versa.

nals and does not present a block diagonal structure. Based on these results, we can see that the proposed shape matching approach is more robust to the presence of noise in shapes as compared to its competitive techniques. Figure 13 presents the retrieval results for some of the query shapes to highlight the effectiveness of the proposed approach as compared to integral invariant and differential invariant. The results retrieved for different query shapes using CRISM, differential and integral invariant are presented in bottom, center and top row respectively.

We now demonstrate the performance of CRISM using other publicly available datasets including Chicken, Diatom and MixedBag datasets. This will allow us to directly compare with a variety of published work that has reported the performance of their shape matching approaches using identical experiment. Comparative evaluation is provided in terms of 1-NN classification accuracies obtained using leave-one-out cross-validation. Table 2 shows the classification accuracies of CRISM using different datasets.

Experiment on chicken dataset enables us to compare directly with [2] and [43] who report the classification accuracy of 80.04% and 79.5% respectively. The shape matching approach specified in [43] takes around a minute for one to one

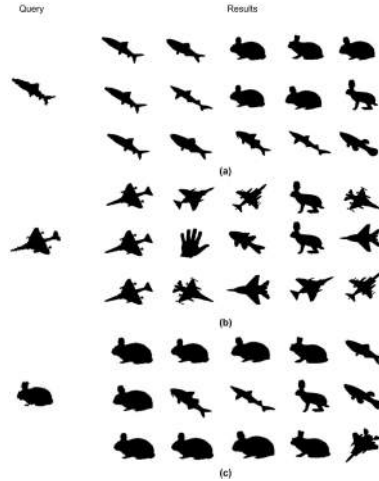


Fig. 13. Illustrative results for 5-NN queries on silhouette dataset (a) Query 1 (b) Query 2 (c) Query 3.

Dataset	# of Samples	# of classes	% Classification Accuracy
Diatom	781	37	72.73
Chicken	446	5	80.71
MultiBag	160	9	95.625

Table 2

Classification accuracies of CRISM using several publicly available shape datasets.

shape matching whereas [2] reported an average time of 0.0039 seconds. On the other hand, shape matching using CRISM takes an average time of  $2.709 \times 10^{-4}$  seconds and still provides a better retrieval accuracy. Similarly, [2] reported the classification accuracy of 72.47% for Diatom dataset whereas CRISM achieved the classification accuracy of 72.73% although CRISM-based shape matching is 2 orders of magnitude faster than the shape matching approach proposed in [2]. MixedBag dataset allows us to compare with [44] who utilize Chamfer and Hausdorff based distance measures. They reported an accuracy of 94% and 93% accuracy with Chamfer and Hausdorff distance respectively. On the other hand, [2] reported the classification accuracy of 95.625% which is same as the accuracy achieved by our proposed approach.

Overall, the experiment demonstrates the superiority of proposed CRISM-based shape matching as compared to other approaches, both w.r.t. efficiency and accuracy. Although CRISM is at least two order or magnitude faster than its closest competitor, it still provides similar or better retrieval accuracies than competitive techniques for variety of shape datasets.

### 6.3 Efficiency Experiments

The purpose of this experiment is to evaluate the performance of proposed shape matching mechanism with respect to time efficiency. We also want to demonstrate the scalability of Indexed\_CRISM (ICRISM) based shape search to the increasing size of shape datasets. To establish the base case, we have implemented wedge and early abandoning techniques as proposed in [2]. [2] use DTW as a distance measure and employs brute-force approach to achieve rotational invariant shape matching. For the proposed ICRISM approach, we have generated hierarchial indexing structure using branching factor  $b^* = 10$  and  $\kappa = 50$  in eq. (15). We tested on the combination of projectile point and hetrogenous dataset [2]. In total, the dataset contains 21,000 samples. We have implemented these algorithms using MATLAB 7 and running times are noted on an Intel Pentium IV 1.73 GHz machine with 1 GB of RAM.

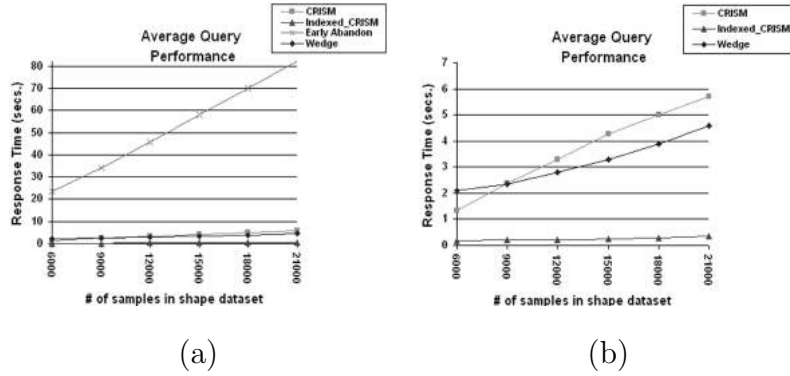


Fig. 14. Average retrieval time to answer a 100-NN query for varying number of samples in shape dataset (a) using four different algorithms (b) using three best algorithms.

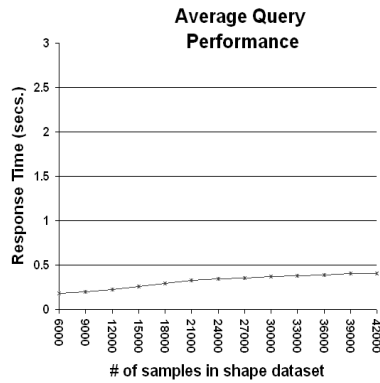


Fig. 15. Average retrieval time to answer a 100-NN query for varying number of samples in modified shape dataset using ICRISM.

Each sample is removed from the dataset one by one and is treated as a query. Average query time required to answer 100-NN query using CRISM,

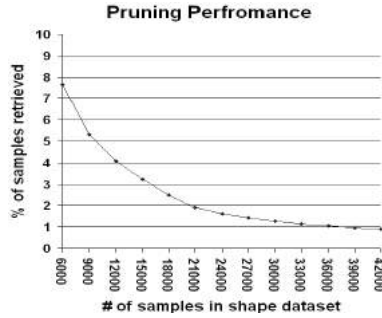


Fig. 16. Average percentage of samples retrieved to answer 100-NN query using modified shape datasets of different sizes.

ICRISM, early abandoning and wedge are presented in Figure 14. We can see that the proposed ICRISM based shape matching performs significantly better than other approaches followed by wedge-based search as proposed in [2]. It is interesting to see that CRISM based sequential shape matching is also quite efficient and gives competitive performance to wedge even without utilizing any pruning mechanism. On the other hand, early abandoning performs the worst and is not scalable to large datasets. The superior performance of ICRISM as compared to CRISM is attributed to the pruning power of DBS using proposed indexing structure. To evaluate the scalability of ICRISM to larger datasets, we double the size of dataset by making its copy and inducing noise in the shapes using noise induction mechanism as specified in Experiment 1. We set  $\sigma = 4.0$  to simulate high level noise in shapes. The modified dataset now contains 42,000 samples in total. Average query time using ICRISM for modified dataset is shown in Figure 15. It can be seen that ICRISM efficiency remains consistent irrespective of the number of samples in the dataset. To highlight the pruning capability of ICRISM, we counted the fraction of shapes that must be retrieved from the modified dataset in order to perform shape matching while ensuring no false negatives. The percentage of samples retrieved to execute 100-NN query for datasets of different sizes are presented in Figure 16. It is evident from the results in Figure 16 that the percentage of samples retrieved for shape matching using ICRISM decreases with increase in the size of dataset. The pruning capability of proposed approach is especially useful in situations where datasets are large enough not to fit in the main memory and minimizing disk accesses is key for efficient shape matching.

As a final sanity check to ensure that the pruning mechanism proposed in ICRISM does not result in false negatives, we matched the search results obtained using CRISM and ICRISM based search mechanisms. The search results obtained using ICRISM approach is exactly identical to the one obtain using simple CRISM-based search which is an experimental proof of the exact indexing capability of ICRISM for a given  $k$ -NN query.

## 7 Discussion and conclusions

In this paper, we have discussed shape matching in the presence of noise and other distortions such as articulation and rotation. A CRISM algorithm has been proposed that exploits the contour information for shape matching. Contours are converted into normalized centroid distance based time series and is modeled using orthogonal basis coefficient feature space representation. We have compared the performance of different dimensionality reduction techniques. DFT has been selected as dimensionality reduction mechanism as it gives overall best results in real time situations where shapes are susceptible to high level of noise. Mapping shape contours from point sequences to DFT coefficient feature space improves retrieval efficiencies. A critical-point based approach to support efficient rotation-invariant shape matching is presented. The proposed algorithm is robust to affine transformations and other arbitrary distortions. A major contribution of this paper is a novel hierarchical tree based indexing method for speeding up retrieval in any feature space that contains feature vector of equal length. In this paper, we have applied the proposed indexing structure to CRISM-based shape matching, namely ICRISM, which makes it scalable to increasingly large shapes datasets. ICRISM supports fast shape matching in the presence of very large datasets while guaranteeing identical results to the one obtained using sequential CRISM.

Experimental results are presented to show the robustness of CRISM-based approach for shape matching in the presence of increasing amount of noise. Experiment performed on silhouette dataset (containing 216 samples) shows that CRISM gives better retrieval accuracies than competitive techniques such as differential invariants and integral invariants under perturbation in the presence of different noise levels. Experiments performed on Diatom (781 samples), Chicken (446 samples) and Multibag (160 samples) datasets demonstrates that CRISM gives similar or better retrieval accuracies than [2][43][44] although the proposed approach is 2 orders of magnitude faster than the closest competitor [2]. It has also been shown that the proposed ICRISM based shape matching approach dramatically further speeds up CRISM while ensuring no false negatives and outperforms competitive techniques w.r.t. retrieval accuracy and efficiency.

## References

- [1] R. Osada, T. Funkhouser, B. Chazelle, D. Dobkin, Shape Distributions. ACM Transactions on Graphics, vol. 21, no. 4, October, 2002, pp. 807-832.
- [2] E. Keogh, L. Wei, X. Xi, S-H. Lee, M. Vlachos, LB-Keogh Supports Exact Indexing of Shapes under Rotation Invariance with Arbitrary Representations

and Distance Measures, VLDB, 2006.

- [3] T. Adamek, N. E. OConnor, A multiscale representation method for nonrigid shapes with a single closed contour, *IEEE Circuits and Systems for Video Technology*, vol. 14, no. 5, 2004, pp. 742-753.
- [4] T. Adamek, N. E. OConnor, Efficient contour-based shape representation and matching, *Multimedia Information Retrieval*, 2003, pp. 138-143.
- [5] E. Attalla, P. Siy, Robust shape similarity retrieval based on contour segmentation polygonal multiresolution and elastic matching, *Pattern Recognition*, vol. 38, no. 12, pp. 2229-2241, 2005.
- [6] C. Faloutsos, M. Ranganathan, Y. Manolopoulos, Fast Sub-sequence Matching in Time-Series Databases, *Proceedings of the 1994 ACM SIGMOD International Conference on Management of Data*, 1994, pp. 419-429.
- [7] R. Agarwal, C. Faloutsos, A. Swami, Efficient Similarity Search in Sequence Databases, *4th International Conference of Foundations of Data Organization and Algorithms*, Evanston, Illinois, USA, October 1993, pp. 69-84.
- [8] K. Chan, A. Fu, Efficient time series matching by wavelets, *Proc. of International Conference on Data Engineering*, Sydney, March 1999, pp. 126-133.
- [9] E. Keogh, K. Chakrabarti, M. Pazzani, S. Mehrota, Locally adaptive dimensionality reduction for indexing large time series databases, *Proc. ACM SIGMOD Conference*, 2001, pp. 151-162.
- [10] Y. Cai, R. Ng, Indexing Spatio-Temporal Trajectories with Chebyshev Polynomials, *ACM SIGMOD/PODS Conference*, France, June 13-18, 2004, pp. 599-610.
- [11] G. Mori, S. Belongie, J. Malik, Efficient Shape Matching using Shape Contexts, *IEEE Transactions on Pattern Analysis and Machine Intelligence*, vol. 27, no. 11, pp. 1832-1837, November 2005.
- [12] S. Belongie, J. Malik, J. Puzicha, Shape Matching and Object Recognition using Shape Contexts, *IEEE Transactions on Pattern Analysis and Machine Intelligence*, vol. 24, no. 24, pp. 509-522, April 2002.
- [13] S. Belongie, J. Malik, J. Puzicha, Matching shapes, *Proceedings of Eighth IEEE International Conference on Computer Vision*, Vol. I, Vancouver, Canada, pp. 454-461, July 2001.
- [14] E. R. Davies, *Machine Vision: Theory, Algorithms, Practicalities*, Academic Press, New York, pp. 171-191, 1997.
- [15] S. Manay, D. Cremers, B-W. Hong, A. J. Yezi, S. Soatto, Integral Invariants for Shape Matching, *IEEE Transactions on Pattern Analysis and Machine Intelligence*, vol. 28, no. 10, pp. 1602-1618, October 2006.

- [16] A. M. Bruckstein, R. J. Holt, A. N. Netravali, T. J. Richardson, Invariant Signatures for Planar Shape Recognition under Partial Occlusion, *Journal of Computer Vision, Graphics, and Image Processing*, vol. 58, no. 1, pp. 49-65, 1993.
- [17] M. Boutin, Numerically Invariant Signature Curves, *Journal of Computer Vision*, vol. 40, no. 3, pp. 235-248, 2000.
- [18] A. W. Fu, E. Keogh, L. Y. H. Lau, C. A. Ratanamahatana, Scaling and Time Warping in Time Series Querying, *VLDB*, vol.14, no.5, pp.742-753, 2005.
- [19] D. Chetverikov, Y. Khenokh, Matching for shape defect detection, *Lecture Notes in Computer Science*, Vol. 1689, Springer, Berlin, pp. 367374, 1999. E.R. Davies, *Machine Vision: Theory, Algorithms*, E.R.
- [20] S. Berretti, A.D. Bimbo, P. Pala, Retrieval by shape similarity with perceptual distance and ejective indexing, *IEEE Transaction on Multimedia*, vol. 2, no. 4, pp. 225239, 2000.
- [21] G. Dudek, J.K. Tsotsos, Shape representation and recognition from multiscale curvature, *Journal of Computer Vision and Image Understanding*, vol. 68, no. 2, pp. 170189, 1997.
- [22] D. Li, S. Simske, Shape Retrieval Based on Distance Ratio Distribution, *HP Tech Report HPL-2002-251*, 2002.
- [23] A. Cardone, S. K. Gupta, M. Karnik, A survey of shape similarity assessment algorithms for product design and manufacturing applications, *ASME Journal of Computing and Information Science in Engineering*, vol. 3, no. 2, pp. 109-118, 2003.
- [24] R. Osada, T. Funkhouser, B. Chazelle, D. Dobkin, Shape Distributions, *ACM Transactions on Graphics*, vol. 21, no. 4, pp. 807-832, October, 2002.
- [25] T. Adamek, N. E. OConnor, A multiscale representation method for nonrigid shapes with a single closed contour, *IEEE Circuits and Systems for Video Technology*, vol. 14, no. 5, pp. 742-753, 2004.
- [26] Z. Wang, Z. Chi, D. Feng, Q. Wang, Leaf Image Retrieval with Shape Features, In *Proceedings of the 4th International Conference on Advances in Visual Information Systems*, pp 477- 487, 2000.
- [27] B. Bhanu, X. Zhou, Face recognition from face profile using dynamic time warping, In *Proceedings of International Conference on Pattern Recognition*, pp. 499-502, 2004.
- [28] X. Wang, L. Ye, E. Keogh, C. Shelton. Annotating Historical Archives of Images, *8th ACM/IEEE-CS Joint Conference on Digital libraries*, pp. 341-350, 2008.
- [29] E. J. Keogh, M. J. Pazzani, A simple dimensionality reduction technique for fast similarity search in large time series databases, *Pacific-Asia Conference on Knowledge Discovery and Data Mining*, 2000, pp. 122-133.

- [30] F. I. Bashir, A. A. Khokhar, D. Schonfield, A hybrid system for affine-invariant trajectory retrieval, In Proc. MIR'04, pp. 235-242, 2004.
- [31] S. Khalid, A. Naftel, Evaluation of matching metrics for trajectory based indexing and retrieval of video clips, Proceedings of IEEE WACV, Colorado, USA, January 2005, pp. 242-249.
- [32] E. Keogh, K. Chakrabarti, M. Pazzani, S. Mehrota, Dimensionality reduction for fast similarity search in large time series databases, Journal of Knowledge and Information Systems, 2000.
- [33] E. J. Keogh, Exact indexing of dynamic time warping, In Proc. Of 28th International Conference on Very Large Data Bases, pp. 406-417, 2002.
- [34] S. Kim, S. park, W. Chu, An indexed based approach for similarity search supporting time warping in large sequence databases, In Proceedings of 17th International Conference on Data Engineering, pp. 607-614, 2001.
- [35] D.G. Lowe, Distinctive Image Features from Scale-Invariant Keypoints, International Journal on Computer Vision, vol. 60, no. 2, pp. 91-110, 2004.
- [36] E. G. M. Petrakis, E. Milios, Efficient retrieval by shape content, Proceedings of ICMCS, vol. 2, pp. 616-621, 1999.
- [37] K. L. Tan, B. C. Ooi, L. F. Thiang, Indexing shapes in image databases using the centroid-radii model, Data and Knowledge Engineering, vol. 32, pp.271-289, 2000.
- [38] K. Grauman, T. Darrell, The pyramid match kernel: Discriminative classification with sets of image features, Proceedings of ICCV, 2005.
- [39] J. Philbin, O. Chum, M. Isard, J. Sivic, A. Zisserman, Object retrieval with large vocabularies and fast spatial matching, In CVPR 2007.
- [40] J. Sivic, A. Zisserman, Video google: a text retrieval approach to object matching in videos, In ICCV, 2003.
- [41] E. J. Keogh, M. J. Pazzani, Scaling up dynamic time warping for data mining applications, In Proceedings of the 6th ACM SIGKDD International Conference on Knowledge Discovery and Data Mining, Boston, USA., pp. 285-289, August 2000.
- [42] <http://www.lems.brown.edu/vision/researchAreas/SIID/silhouette-database.tar.gz>
- [43] R. A. Mollineda, E. Vidal, F. Casacuberta, Cyclic Sequence Alignments: Approximate Versus Optimal Techniques In International Journal of Pattern Recognition and Artificial Intelligence (IJPRAI), vol. 16, no. 3, pp. 291-299, 2002.
- [44] M. Vlachos, Z. Vagena, P. S. Yu, V. Athitsos, Rotation invariant indexing of shapes and line drawings, Proceedings of ACM Conference on Information and Knowledge Management (CIKM), pp. 131-138, 2005.